Journal of Applied Polymer Science

Effect of kaolin nanofiller and processing conditions on the structure, morphology, and biofilm development of polylactic acid

Edwin A. Segura González,[1] Dania Olmos,[1] Gustavo González-Gaitano,[2] Belén Orgaz,[3] Javier González-Benito[1]

[1]Department Materials Science and Engineering and Chemical Engineering and IQMAAB, Universidad Carlos III de Madrid, Av. Universidad 30, 28911 Leganés Madrid, Spain

[2]Departamento de Química y Edafología, Universidad de Navarra, 31080 Pamplona, Spain

[3]Department of Food Science and Technology, Faculty of Veterinary, University Complutense of Madrid, 28040 Madrid, Spain

Correspondence to: J. G. Benito (E-mail: javid@ing.uc3m.es)

ABSTRACT: The effect of high energy ball milling, HEBM, and the presence of kaolin on the structure, morphology, and biofilm development of polylactic acid, PLA, were studied. Biofilm development was evaluated in terms of structural and/or morphological variations so as the sole presence of kaolin. Composites based on PLA filled with kaolin were prepared by HEBM followed by hot pressing to obtain films. Structure was studied by X-ray diffraction and Fourier transformed infrared spectroscopy whereas morphology was inspected by scanning electron microscopy and atomic force microscopy. To study biofilm development on the surface of these materials, *Pseudomonas fluorescens* B52 were used. The shear forces from the milling process favor kaolin dispersion within the PLA. Longer milling times and cryogenic conditions improve clay dispersion. Subsequent hot pressing process enhances the most ordered structure of PLA (α-phase) which is also favored with previous milling at longer times and under cryogenic conditions. Changes in *P. fluorescens* biofilm development are mainly due to modifications of surface properties induced by structural variations, being the most ordered structures those which better support bacterial adhesion and proliferation. © 2015 Wiley Periodicals, Inc. J. Appl. Polym. Sci. **2015**, *132*, 42676.

KEYWORDS: biofilm development; high energy ball milling; kaolin; nanocomposites; polylactic acid

Received 12 April 2015; accepted 29 June 2015

DOI: 10.1002/app.42676

INTRODUCTION

Polymer nanocomposites are a particular kind of materials in which an inorganic phase with at least one nanoscopic dimension (less than 100 nm) is usually dispersed within a polymer. Up to the present moment many studies have shown clear improvements of certain physical or chemical properties. Perhaps the most extended general reason for those changes is the fact that nanosized domains have large surface to volume ratio, which increases the interfacial forces and therefore the general contribution of the so-called interphase zone to the properties of the composite. Among this kind of materials, polymer/clay nanocomposites are receiving much attention due to their interesting mechanical, thermal, and gas barrier properties.[1–3]

Currently, the vast majority of plastics are made from petroleum-based synthetic polymers that do not degrade in a natural environment and their disposal leads to serious environmental problem. A sustainable alternative is to design biodegradable polymer nanocomposites. Probably the easiest way to achieve the above-mentioned is to use, as main constituent of the composites, biodegradable-based polymer matrices. Among them PLA has been used as an important bio-based polymer in the biomedical and environmental applications due to its biodegradability, biocompatibility, and non-toxicity.[3–5] Besides, PLA is one of the most promising biopolymers as it is commercially available, relatively cheap, and presents a good balance between processability and final performance.[5,6]

Many of the applications of PLA based polymers are centered in food industry (short-term packaging)[6] or biomedical industry (sutures, drug encapsulation, or drug delivery).[7–9] In such materials, antimicrobial activity can be considered one of the most innovative ways to improve their performance. In the case of food packaging microbial growing inhibition assess food safety as well as quality and freshness during the entire shelf-life of the product. Thus, when fillers are incorporated within polymers for biomedical or food packaging applications, microbiological activity should be studied. Hence, these biodegradable polymers may play a dual role respect to the interaction with microorganisms: (i) they are expected to inhibit growing of

© 2015 Wiley Periodicals, Inc.

non-desired bacteria (pathogens and food spoilage microorganisms) while (ii) microorganisms causing final degradation of waste materials should be minimally altered.

However, there are properties such as flexibility, gas barrier properties, and high melt viscosity during processing, which are often not good enough for some end-use applications, such as blow molding.[10,11] In this sense, to improve physical properties of PLA, especially in terms of thermomechanical stability, addition of different fillers (nanoparticles) was explored.[12] In general, an adequate dispersion of nanoparticles should be ensured to improve successfully the polymer properties when nanofillers are used.[13] In fact, when layered silicate is uniformly dispersed and exfoliated into a polymer matrix, the polymer properties can improve to a dramatic extent.[14–18] A poor dispersion of nanoparticles usually yields aggregates or even agglomerates of tens of microns, reducing therefore the surface to volume ratio and the effective interaction between the matrix and the filler. The degree of dispersion of clay platelets into polymer matrices usually determines the microstructure of the nanocomposites and therefore their properties. In this sense, two main idealized types of polymer–clay morphologies, intercalated and exfoliated, can be identified. The intercalated structure results from penetration of a few polymer chains into the silicate interlayer, whereas exfoliation yields complete separation between platelets. In general, the best improvements in a property and the least influence to viscosity for low molecular weight suspensions result from the exfoliated morphologies. Therefore, to control the way of dispersing nanofillers within polymer matrices is of primary importance.

Up to now, several options have been investigated to attain the best dispersion of nanoparticles in polymers. Among them, the use of organomodified particles can be highlighted when a better compatibility between the constituents of the composites is wanted.[19] After preparing the modified filler, conventional methods of polymer processing might be used (extrusion, injection molding, hot pressing, ...). However, modification of nanoparticles can be difficult, time-consuming, and expensive. Therefore, new methods of processing should be found to avoid the first step of nanoparticle modification. In the last decade, different studies point out that high energy ball milling, HEBM, is a very promising method to mix nanoparticles with thermoplastic polymers to finally obtain a uniform dispersion of the filler within the polymer matrix.[13,20–23]

PLA/kaolin nanocomposites are of particular interest as kaolin, the most abundant clay mineral, is mainly formed by kaolinite. Kaolinite ($Al_2Si_2O_5(OH)_4$) is a 1 : 1 phyllosilicate whose layers are composed of tetrahedral and octahedral sheets linked together by hydrogen bonds. Although some attempts have been made to investigate polymer/kaolin composites in-depth studies about its structure and morphology should be performed to correlate them, with microbiological activity.[24]

In this work, polylactic acid, PLA, filled with kaolin nanoclay was investigated. In particular, the effect of HEBM (used to disperse the nanofiller) so as the proper presence of kaolin nanofiller on the structure, morphology, and thermal properties was studied. Changes in the microbiological activity of the nanocomposites were analyzed to understand whether they come from structural and morphological variations or from the presence of kaolin.

EXPERIMENTAL

Materials and Methods

Materials. Polylactic acid (PLA) was provided by Resinex Spain, SL, and manufactured by Nature Works LLC (Ref. code: PLA Polymer 7032D; glass transition temperature, $T_g = 55–60°C$; melting temperature, $T_m = 160°C$; and processing temperature 200–220°C). To prepare the polymer nanocomposites highly crystalline kaolin supplied by Sigma Aldrich (K7375) was used as filler (chemical composition: 46.54% SiO_2; 39.5% Al_2O_3; and 13.96% H_2O). For the microbiological studies, tryptic soy broth (TSB), tryptic soy agar (TSA), and peptone water were purchased from Sigma Aldrich. TSB and TSA were used as the bacterial growth medium.

Samples Preparation. Polymer nanocomposites were prepared from two steps: (i) HEBM process to blend polylactic acid (PLA) with kaolin particles; and (ii) hot pressing to finally obtain nanocomposites in the form of films. The amount of filler was set at 20 wt %.

To evaluate the effect of milling time and temperature, three processing conditions were considered (HEBM at room temperature [rt] for 1 h and 2 h of active milling, respectively, and HEBM under cryogenic conditions for 1 h of active milling). For milling at rt conditions a 6 Fritsch Pulverisette miller was used with 11 steel balls of 15 mm of diameter. Milling conditions were set to 350 rpm using cycles of 10 min of active milling plus 3 min of resting. When cryogenic milling was performed, a Retsch MM400 mixer mill was used. The milling conditions were set at a frequency of 25 Hz for 5 min using a stainless steel ball of 25 mm of diameter. Every 5-min cycle of active milling, the samples were immersed in liquid nitrogen for 15 min to ensure cryogenic conditions. The entire process is repeated as many times as necessary to reach the desired active milling time, 1 h in this work. For comparison purposes, pure materials, PLA and kaolin, were separately milled under the same milling conditions as those used in the PLA–kaolin mixtures.

Finally, materials in the form of films were obtained by hot pressing. Powders from the milling process were sandwiched in-between two glass plates (previously coated with Frekote NC-44 as demoulder) with an applied load of about 14 N/cm^2. Then, the sandwiched samples were put in an oven at 190°C for 1 h. The prepared films were stored in a desiccator to prevent moisture absorption.

Table I gathers the nomenclature used. Polylactic acid (PLA); kaolin (K); film (F); milled for 1 h (M1); milled for 2 h (M2); cryogenic milling process (C1).

Experimental System for Biofilm formation. *Pseudomonas fluorescens* B52 first isolated from refrigerated raw milk (Richarson and Tewhaki, año) was used as biofilm model organism. Strains were stored in trypticase soy broth (TSB, Oxoid) with 15% glycerol at −20°C. Preinocula were cultured overnight in TSB at 30°C. Cells were harvested by centrifugation at 4000 × *g* for

Table I. Samples Codes and Conditions of Sample Preparation

Sample code	HEBM (type)	Nanofiller (Kaolin 20 wt %)	Film (hot pressing)
PLA	NO	NO	NO
PLA-F	NO	NO	YES (190°C, 1 h)
PLA-M1	YES (rt, 1 h)	NO	NO
PLA-M1F	YES (rt, 1 h)	NO	YES (190°C, 1 h)
PLA-M2	YES (rt, 2 h)	NO	NO
PLA-M2F	YES (rt, 2 h)	NO	YES (190°C, 1 h)
PLA-C1	YES (cryo, 1 h)	NO	NO
PLA-C1F	YES (cryo, 1 h)	NO	YES (190°C, 1 h)
K	NO	NO	NO
K-M1	YES (22°C, 1 h)	NO	NO
K-M2	YES (22°C, 2 h)	NO	NO
K-C1	YES (cryo, 1 h)	NO	NO
PLA-M1K	YES (22°C, 1 h)	YES	NO
PLA-M1KF	YES (22°C, 1 h)	YES	YES (190°C, 1 h)
PLA-M2K	YES (22°C, 2 h)	YES	NO
PLA-M2KF	YES (22°C, 2 h)	YES	YES (190°C, 1 h)
PLA-C1K	YES (cryo, 1 h)	YES	NO
PLA-C1KF	YES (cryo, 1 h)	YES	YES (190°C, 1 h)

10 min, washed twice in sterile TSB, and their OD_{600} adjusted by dilution with TSB to be used as inoculum, starting the cultures with a cell density of 10^3 CFU/mL.

Biofilms were cultivated at 30°C in disposable 24-well microplates (Thermo Fisher Scientific) on the previously prepared nanocomposites materials. Before developing biofilms, the materials in the form of films with areas of about 1 cm^2 were autoclaved at 121°C for 15 min. After that, in each well of the microplate one sterile film-coupon was immersed into 1 mL of the corresponding bacterial suspension. The system was incubated under continuous agitation at 80 rpm and 30°C. After 24 h, films were removed, rinsed with saline solution to detach weakly attached cells. Some samples were immediately scanned by atomic force microscopy (AFM) while others were used for cell recovery and counting. For this, attached cells from each coupon were removed using a cotton swab. Cells were then transferred into a 1.5 mL peptone water tube that was vigorously stirred in a vortex to break up cell aggregates, diluted in peptone water, and plated into general medium (Tryptone Soy Agar, TSA, Oxoid). PLA films without kaolin served as a control group. Tests were performed at least twice.

Experimental Techniques and Methods. Crystalline structure of milled samples in the form of powders and films was studied by X-ray diffraction, XRD in the range 3–50° in 2θ, using a Phillips X'Pert X ray diffractometer with a $CuK_{\alpha 1}$ ($\lambda = 0.15406$ nm) anode tube at the standard conditions of 40 kV and 40 mA. A rectangular sample holder with dimensions 1 × 2 × 0.1 cm^3 was used. Samples in the form of powder were placed on glass slides promoting random orientation of the crystal fragments. X-ray diffraction was performed in different areas of each sample to verify reproducibility.

Fourier transformed infrared (FTIR) spectra were recorded using an ATR-FTIR Nicolette Avatar 360 at room temperature from 600 to 4000 cm^{-1} by averaging 32 scans at a resolution of 2 cm^{-1}. Data treatment was performed with OMNIC E.S.P. v5.1 software (Nicolet).

The inspection of the morphology in terms of particle dispersion was performed using a PhilipsXL30 scanning electron microscope. Domains with different elemental compositions were imaged using backscattered electrons signal, BSE. To avoid charge accumulation on the samples, gold coating by sputtering from anodic deposition was performed.

Topography of films at nanoscale was inspected by AFM using a Nanoscope IV System from Digital Instruments. A triangular micro-fabricated cantilever with a length of 125 μm, 0.01–0.025 Ω cm Antimony (n) doped Si, and a nominal spring constant of 20–80 N/m was used. A resonance frequency of the cantilever typically at 320 kHz was chosen for the tapping mode oscillation. Moderate tapping forces were used by setting the set-point ratio between 0.6 and 0.7. The AFM images were obtained with a maximum scan range of 20 × 20 μm^2.

RESULTS AND DISCUSSION

Figure 1 shows photographs of the films prepared. It can be clearly observed that only when cryogenic conditions are used the nanocomposite samples macroscopically show a uniform dispersion of kaolin particles. On the contrary, when milling was performed at room temperature, regions of higher concentration of particles are formed [Figure 1(b,c)], being the dispersion improved when milling time is increased. One probable explanation of these results is the fact that when the samples are prepared under cryogenic conditions, the grinding jar is cooled in liquid nitrogen and so the sample is embrittled. This embrittlement of the PLA matrix may lead to the formation of smaller size particles of PLA thus allowing a better mixing with the kaolin particles.

As control samples, the pure components of the nanocomposites were subjected to the different treatments in order to check the direct effect of processing on them without counting the influence of the other component.

Clay minerals are characterized by their basal reflections that may vary in response to a particular treatment. Figure 2 shows a comparison between X-ray diffraction patterns of kaolin samples subjected to different treatments. Commercial kaolin shows a maximum diffraction peak at $2\theta = 12.4°$ corresponding to a basal spacing of 0.72 nm, according to Bragg's law ($n\lambda = 2d \sin \theta$), assigned to the crystal planes (0 0 1), and a diffraction peak at $2\theta = 24.9°$ corresponding to a spacing of 0.36 nm, assigned to the (0 0 2) planes. "A" peaks refer to the presence of $H_2KAl_3(SiO_4)_3$ (muscovite), "B" peaks to $Al_2Si_2O_5(OH)_4$ (kaolinite), and "C" peaks to SiO_2 (quartz). Most of the peaks are intense and narrow, which indicates a highly crystalline clay and confirms the abundant amount of kaolinite ($Al_2Si_2O_5(OH)_4$) present in the kaolin used in this study.[25] Besides, other less

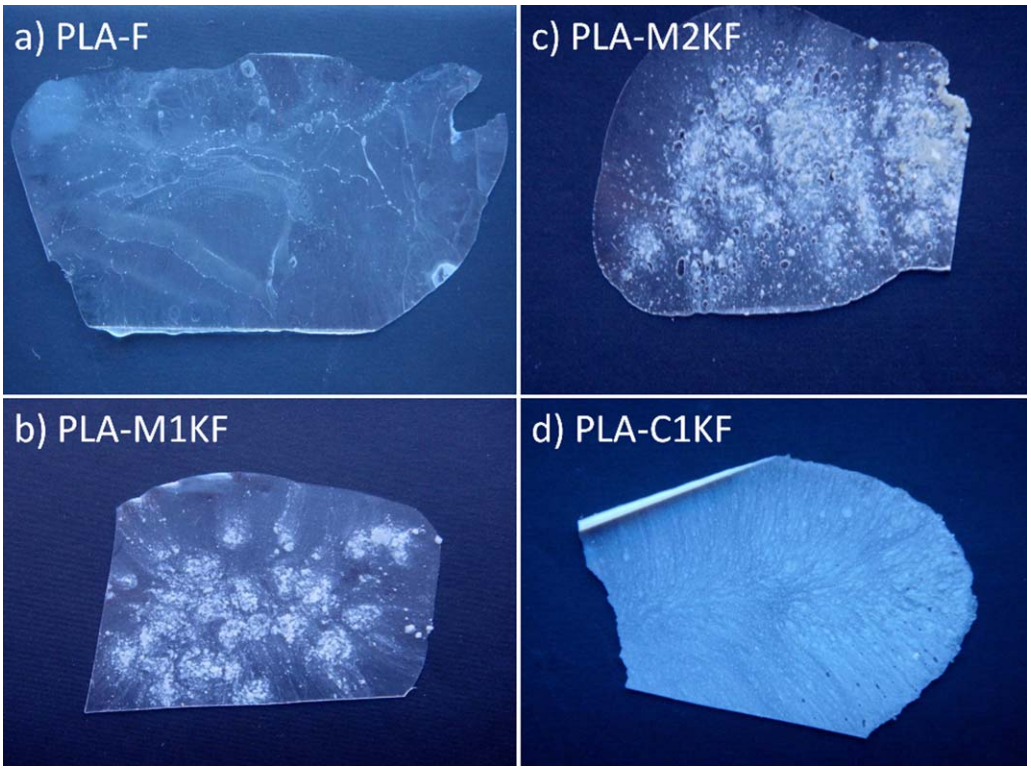

Figure 1. Photographs of samples in the form of films: (a) PLA, (b) PLA/Kaolin nanocomposite (milling at rt for 1 h); (c) PLA/Kaolin nanocomposite (milling at rt for 2 h); (d) PLA/Kaolin nanocomposite (milling under cryogenic conditions for 1 h). [Color figure can be viewed in the online issue, which is available at wileyonlinelibrary.com.]

intense peaks are also observed, corresponding to other interplanar spacings of kaolin.[26] As a result of milling, the intensity of the main peaks decreases, this effect being enhanced with milling time. Conversely, milling temperature showed almost no effect on kaolin structure. Regardless of milling temperature, 1 h of active milling reduces crystallinity of kaolin 38–40% as estimated from the ratio between crystalline peaks area and the crystalline plus amorphous areas in the diffractograms. However 2 h of active milling at room temperature reduce the crystallinity about twice.

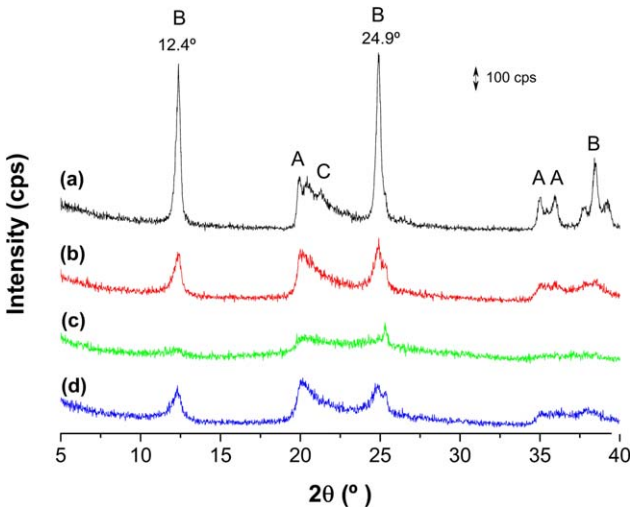

Figure 2. X-ray diffraction patterns of (a) kaolin; (b) kaolin milled for 1 h; (c) kaolin milled for 2 h; and (d) kaolin milled for 1 h under cryogenic conditions. [Color figure can be viewed in the online issue, which is available at wileyonlinelibrary.com.]

Figure 3 shows DRX patterns of PLA in the form of powders [Figure 3(a)] and films [Figure 3(b)], respectively, after different conditions of milling. For comparison, XRD diffractogram of commercial polylactic acid (PLA) was added in both cases.

Commercial PLA has a major crystalline peak at $2\theta = 16.8°$ corresponding to (2 0 0)/(1 1 0) planes of the orthorhombic structure, and lower intensity peaks at $2\theta = 19.1°$; and 22.4° assigned to the reflection planes (2 0 3) and (0 1 5), respectively.[27,28] These reflections are usually indicative of the so-called α' structure, as indicated by Pan *et al.*[29] It is also observed how the milling process affects the PLA structure mainly by decreasing the crystallinity, as it happened with kaolin. However, hot pressing process allows recovering the crystallinity of PLA [Figure 3(b)]. In fact, sharper peaks, as well as the appearance of new ones (for instance at $2\theta = 14.1°$, assigned to 0 1 0 plane[29]) are observed in the XRD patterns of PLA films, indicating a higher structural order, as it is also confirmed by the higher degree of crystallinity estimated by the conventional method of calculating the quotient of the area of the peaks over the total area of the diffractogram. Taken altogether, these data point out the generation of α phase associated to the more ordered and compact structure with respect to the α' phase.[29] Figure 4 shows the XRD patterns of the nanocomposites obtained from different processing conditions either in the form of powder [Figure 4(a)] or in the form of films [Figure 4(b)]. In

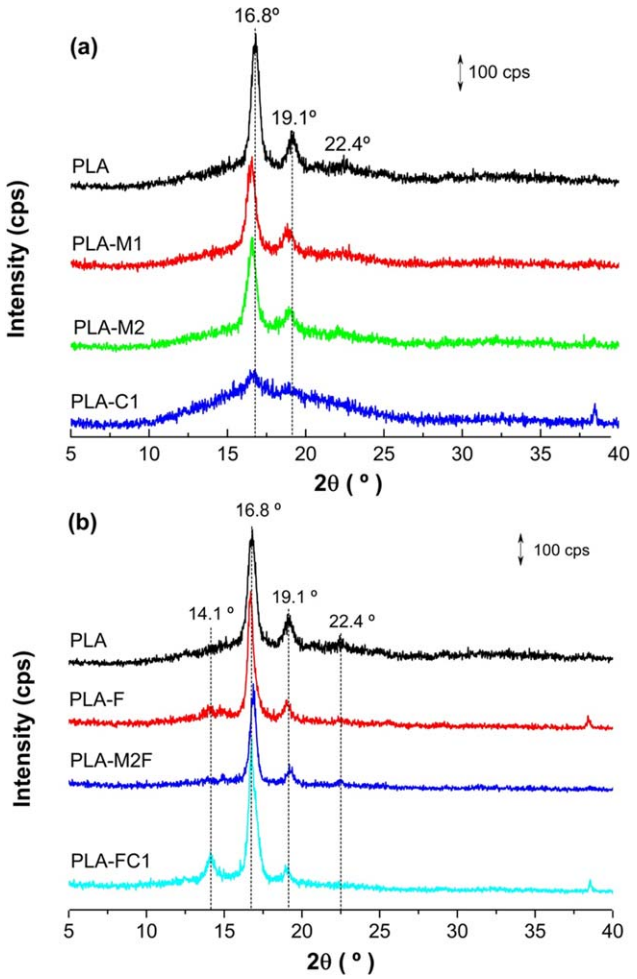

Figure 3. X-ray diffraction patterns of PLA under different processing conditions: (a) powders and (b) films. [Color figure can be viewed in the online issue, which is available at wileyonlinelibrary.com.]

both cases, the traces for commercial kaolin (K) and polylactic acid (PLA) have been added for comparison.

For the samples in the form of powder it is observed how for both PLA and kaolin the crystallinity is highly lost, this effect being more intense when the cryogenic milling was performed. However, after hot pressing, the crystallinity of PLA was clearly recovered and even enhanced, whereas the peaks associated to kaolin keep a relatively lower intensity, which may be an indication of the good dispersion of clay within the PLA, where an important fraction of exfoliated material is expected.

The ATR-FTIR spectra of the samples of kaolin subjected to different treatments are shown in Figure 5. Only in the case of the as received kaolin four bands assigned to the stretching vibrations of the structural OH starting kaolin (K) can be clearly identified at 3690, 3668, 3649, and 3619 cm^{-1}, respectively. All of them correspond to O—H stretching vibrations where: (i) the band at 3690 cm^{-1} can be associated to free —OH groups or external hydroxyls of the kaolin structure; (ii) the band at 3668 cm^{-1} is usually indicative of interlayer hydrogen bonding in which a major component of the bonding is perpendicular to the basal plane; (iii) the band at 3649 cm^{-1} points out OH groups in which the hydrogen end lies in the direction of the vacant octahedral sites, resulting in a bond orientation for which the major component is parallel to the basal plane; and (iv) the band at 3619 cm^{-1} points out the interlayer hydrogen bonding involving two basal hydroxyls of one sheet and the remaining two oxygen of an opposing silica tetrahedron.[30,31] In contrast to XRD results, the well resolved (less overlapping) IR peaks suggest that the mineral is fairly well ordered. IR bands associated to interlayer OH groups (3690, 3668, 3649 cm^{-1}) may change when different molecules are intercalated between sheets of kaolin as new interactions with those molecules can occur; however, the band at 3619 cm^{-1} corresponding to internal OH groups is not usually affected by such processes of intercalation.[31] When milling was performed, resolution of the FTIR peaks in the region 3800–3500 cm^{-1} is reduced, along with the intensity, and there is a small shift in the bands of about 5 cm^{-1} to higher energies, probably indicating the absence of inner OH groups if a considerable amount of the platelet structure of kaolin is destroyed.

Something similar can be said when the IR region from 1300 to 700 cm^{-1} is considered [Figure 5(b)], where the main band assignment corresponds to the bending mode of the inner surface OH

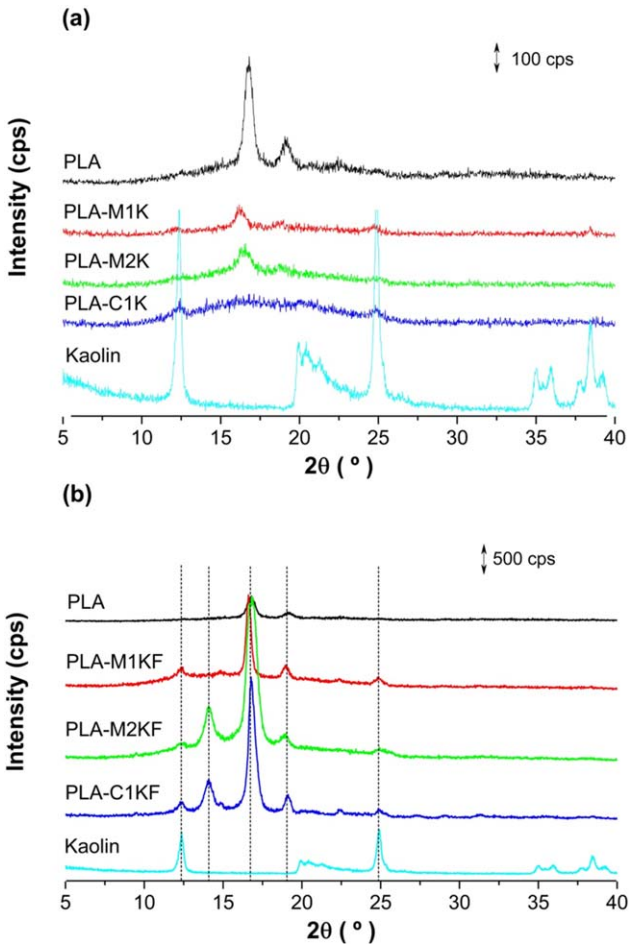

Figure 4. X-ray diffraction patterns of the nanocomposites obtained from different processing conditions: (a) powder and (b) films. [Color figure can be viewed in the online issue, which is available at wileyonlinelibrary.com.]

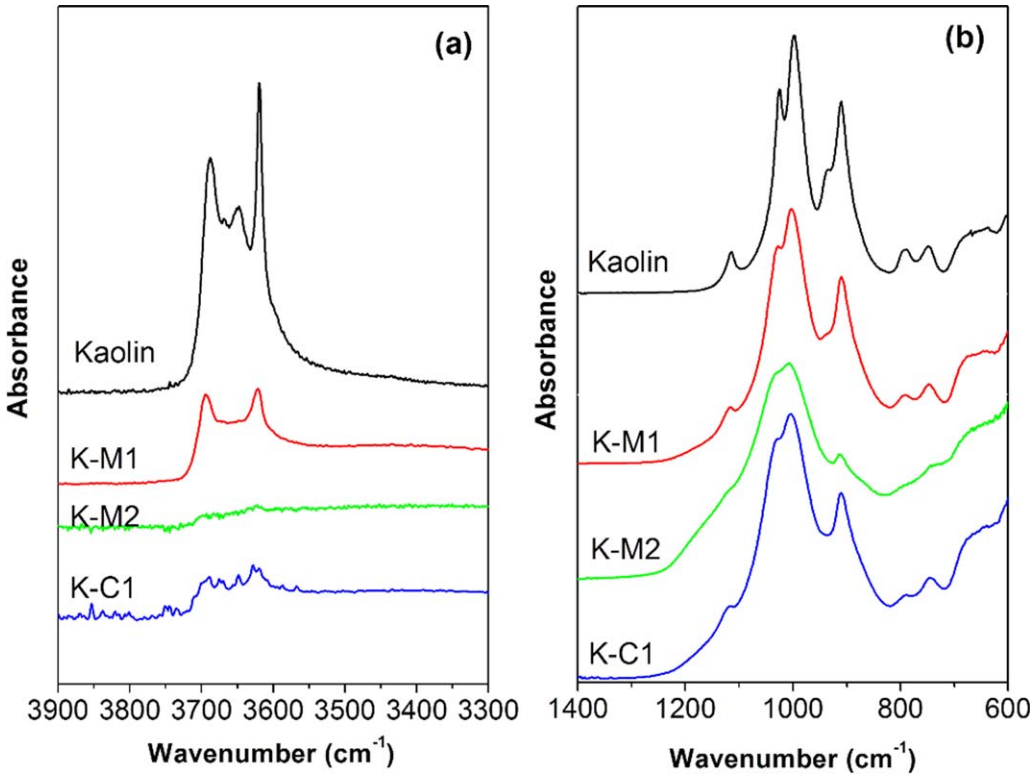

Figure 5. ATR-FTIR spectra of kaolin samples in two different regions. [Color figure can be viewed in the online issue, which is available at wileyonlinelibrary.com.]

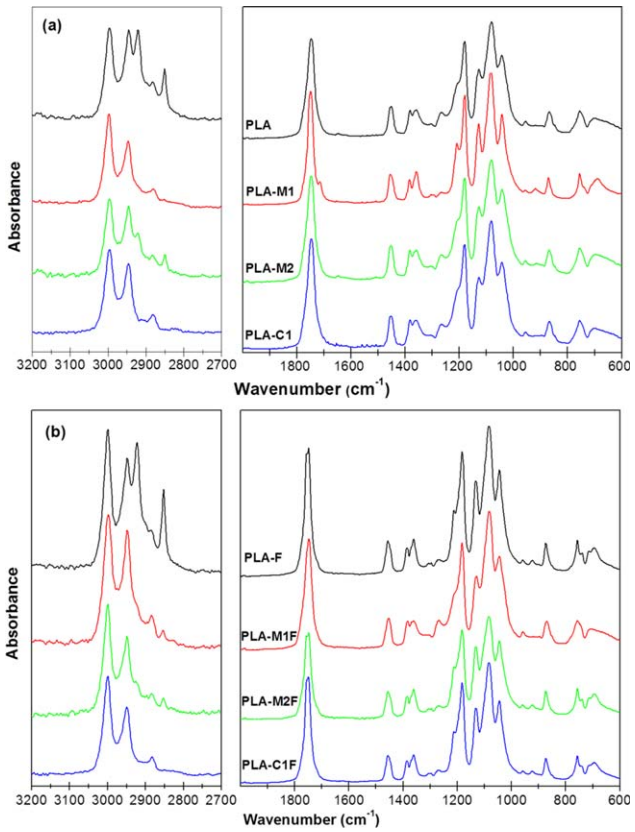

Figure 6. FTIR-ATR spectra of PLA subjected to different treatments: (a) powder and (b) films. [Color figure can be viewed in the online issue, which is available at wileyonlinelibrary.com.]

groups at 913 cm^{-1}, that of the surface OH groups near 936 cm^{-1}; and the Si—O vibration at 1114, 1032, and 1008 cm^{-1}, respectively. Increasing the milling time results in structural damage of kaolin, as can be seen in the less structured spectra [Figure 5(b)] and in the significant reduction of the intensity of the Si—O stretching band at 1114 cm^{-1}, assigned to the newly created product surface. The band at 1025 cm^{-1} may also contain a contribution of muscovite and the peak at 791 cm^{-1} is probably associated with the quartz as an impurity in the kaolin being, according to XRD studies (Figure 2).[31–33] This result completely agrees with that obtained by Frost *et al.* who showed that kaolinite hydroxyls were lost after 10 h of grinding as evidenced by the decrease in intensity of the OH stretching vibrations at 3695 and 3619 cm^{-1} and the deformation modes at 937 and 915 cm^{-1}, concluding that mechanochemical activation (dry grinding) causes the destruction of the crystalline structure of kaolinite by the rupture of the O—H, Al—OH, Al—O—Si, and Si—O bonds.[34]

Figures 6 and 7 show the ATR-FTIR spectra of PLA and PLA–Kaolin nanocomposites for different processing conditions.

It is well known that PLA exhibits mid-IR regions that are highly sensitive to structural changes. Most of those changes are due to transformations between amorphous phase and the α and α' crystalline phases.[29] As it has been already shown, the spectral features in the vibration region of ν_{as}(C—O—C) + ρ_{as}(CH_3), that is, 1260–1160 cm^{-1}, are notably different from the α'- and α-crystals.[29] In general, these results do not evidence significant differences. Only the band centered at about 1210 cm^{-1} seems to be better resolved which might simply point out a higher degree of crystallinity.

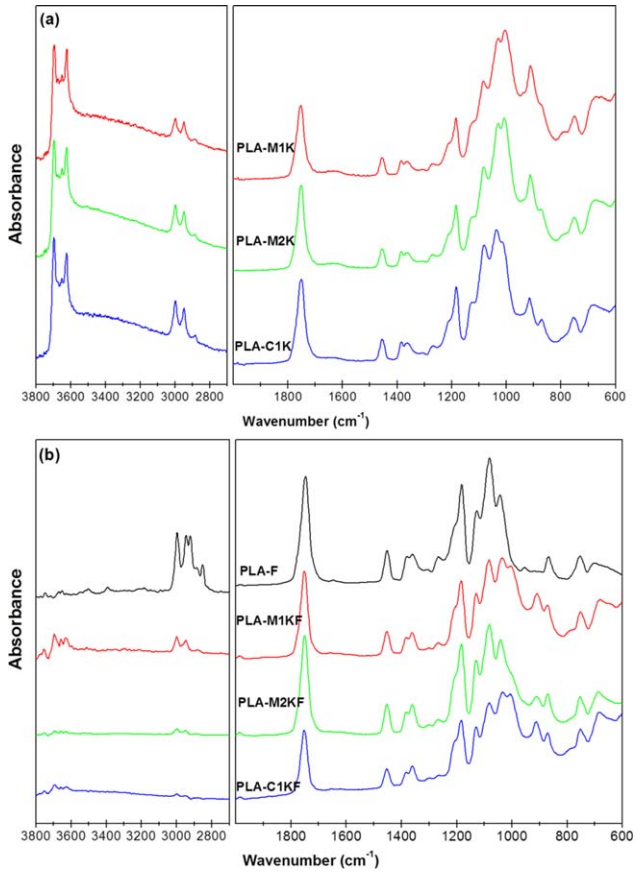

Figure 7. FTIR-ATR spectra of PLA and PLA-K composites subjected to different treatments: (a) powder and (b) films. [Color figure can be viewed in the online issue, which is available at wileyonlinelibrary.com.]

In fact, those samples with a better defined IR peak at 1210 cm^{-1} match those presenting higher ordered structure, as XRD results have shown.

Morphological Characterization

Figure 8 shows the scanning electron microscopy images of the composites under study. In all cases, two domains are clearly discerned, a darker region corresponding to the PLA polymer matrix and a lighter one associated to the kaolin rich phase, as it is formed by heavier elements which yield higher intensity in the BSE signal. By comparing between the samples, three main observations can be made in terms of the uniformity in the dispersion of kaolin. First, when the milling time increases from 1 h to 2 h, kaolin dispersion improves (see, e.g., the comparison between PLA-M1F and PLA-M2F samples). In addition to this, when the milling is performed under cryogenic conditions the kaolin is more uniformly dispersed (compare PLA-M1F and PLA-C1F). Finally, the effect of temperature on the kaolin dispersion is higher than that of the milling time (comparison between PLA-M2F and PLA-C1F).

In terms of particle dispersion, these results are in good agreement with the degree of disorder in the clay filler shown by the XRD and FTIR results and, therefore, with a possible higher exfoliation degree the lower the temperature and the longer the milling time are.

Behavior Under Biofilms Development

Considering the final results in terms of better dispersion of kaolin, the sample of PLA-C1KF was chosen to analyze the effect of the presence of kaolin on the *P. fluorescens* biofilms development. In the other two cases, PLA-M1KF and PLA-M2KF, heterogeneous impact on the biofilm development should occur and consequently the effect of the presence of kaolin would be difficult to evaluate.

Figure 9 shows representative AFM images of *P. fluorescens* biofilms developed on the assayed materials. Attached cell population (number of bacteria per surface unit) considerably increased in those samples obtained by the milling process (PLA-C1KF). These results suggest that biofilm development is more influenced by milling process than by the presence of kaolin (Figure 9).

Microbial counts of samples were also performed 24 h after incubation. A slight increase in bacterial counts was obtained for the samples in the following order: PLA-F (1.6×10^3 CFU/cm^2); PLA-C1F (3.2×10^3 CFU/cm^2); and PLA-C1KF (7.7×10^3 CFU/cm^2), which is in accordance with the AFM observations.

One possible explanation of these results may be the consideration of the differences observed in the polymer structure of the samples under study. In fact, taking into account the results

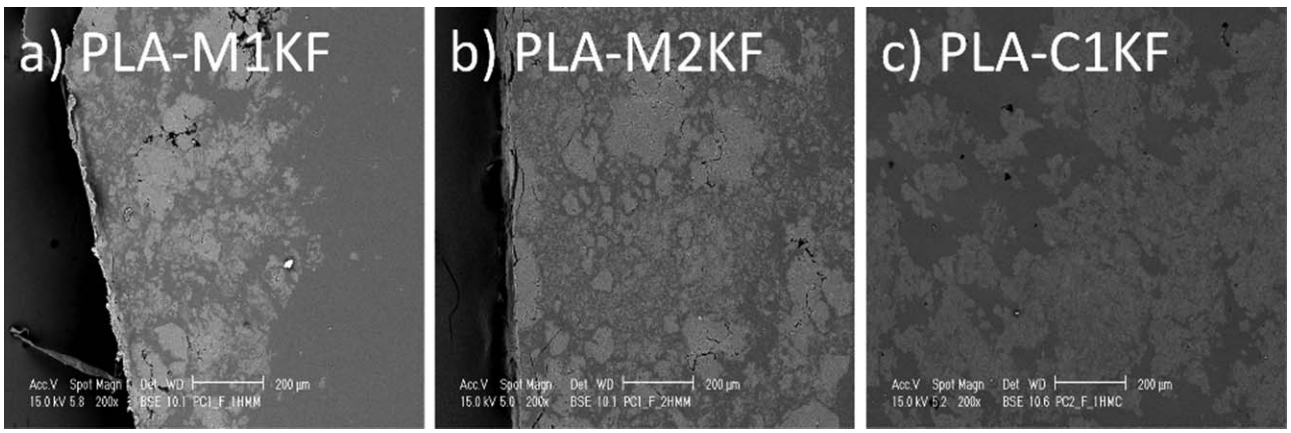

Figure 8. Scanning electronic microscopy of PLA acid film filled with kaolin (20%, w/w): (a) 1 h HEBM; (b) 2 h HEBM; (c) 1 h HEBM under cryogenic conditions.

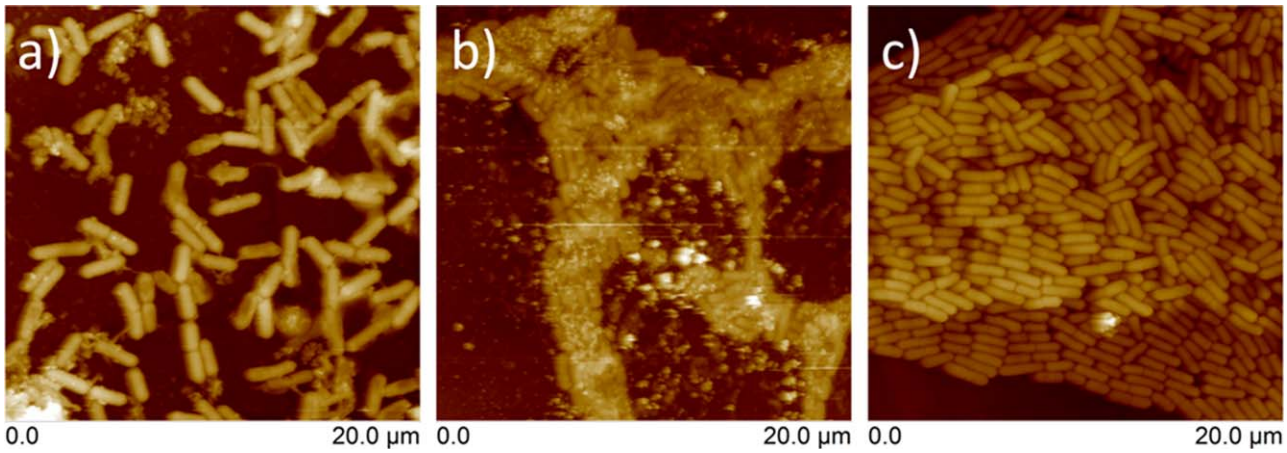

Figure 9. AFM height images for the samples: (a) PLA-F; (b) PLA-FC1; and (c) PLA-FC1K samples subjected to *Pseudomonas fluorescens* culture. [Color figure can be viewed in the online issue, which is available at wileyonlinelibrary.com.]

obtained by XRD and FTIR it is possible to infer that there is a correspondence between the crystalline structure and the bacterial proliferation, the more ordered the structure, the more bacterial proliferation. Therefore, changes in biofilm development in this kind of materials might be due to changes in their surface properties induced by structural variations. The latter would be in accordance with a better adhesion of bacteria to PLA the more ordered the crystalline structure of PLA is. Following the last reasoning one would expect a decrease in bacteria proliferation on PLA based materials by simply decreasing the polymer crystallinity, for instance.

Kaolin itself does not seem to have intrinsic antibacterial activity, as it was also revealed in this work. Unlike other nanoparticles with well-known antibacterial properties such as titania nanoparticles (either in the presence of UV-light or in the absence of light[35]), in the case of kaolin particles the proliferation of microorganisms on the surface of these nanocomposites seems to be enhanced. Based on the above-mentioned, the most reasonable explanation is the structural changes observed due to the milling process. In a previous study,[35] when TiO_2 nanoparticles were introduced in LDPE no significant changes in terms of the degree of crystallinity were observed due to the presence of the particles. Therefore, changes observed in the proliferation and growth of bacteria on the surface of those composite materials were only due to the sole presence of the particles and not to structural or morphological changes introduced in the polymer matrix due to the presence of the particles.

Conversely, in this work, results point out that structural changes caused in PLA matrix due to milling and to the presence of kaolin are favoring the growth of certain bacteria. Even though this may be seen as a disadvantage for PLA based nanocomposites, used for food industry or biomedical industry, these biodegradable polymers should also allow the growth of certain microorganisms to enable their final degradation. Therefore, as a result of this study, we may conclude that depending on processing conditions, the presence of the kaolin in PLA–kaolin nanocomposites may contribute to these composites enabling polymer biodegradation in the presence of certain microorganisms.

CONCLUSIONS

From a preliminary mixing process based on high energy ball milling, composites of PLA/kaolin were prepared. The shear forces applied from the milling process disintegrate the kaolin structure and induce the predominance of the less ordered structure of the α'-phase in the PLA. However, the subsequent hot pressing process enhances the most ordered structure of PLA (α-phase) which, in addition, is favored with previous milling at longer times and under cryogenic conditions. Besides, the more extreme the milling conditions (longer times and lower temperatures), the more uniform the clay dispersion is, pointing out to a higher exfoliation degree of the clay. Finally, it seems that changes in *P. fluorescens* biofilm development were to some extent influenced by the polymer state, being the most ordered structures those which better support bacterial adhesion and proliferation.

ACKNOWLEDGMENTS

The authors gratefully acknowledge financial support from projects MAT2010-16815 and SENACYT doctoral and postdoctoral fellowship from Panama.

REFERENCES

1. Nguyen, Q. T.; Baird, D. G. *Adv. Polym. Technol.* **2006**, *25*, 270.
2. Kiliaris, P.; Papaspyrides, C. D. *Prog. Polym. Sci.* **2010**, *35*, 902.
3. Ray, S. S.; Okamoto, M. *Prog. Polym. Sci.* **2003**, *28*, 1539.
4. Tsuji, H. In Biopolymers for Medical and Pharmaceutical Applications; Steinbüchel, A.; Marchessault, R. H., Eds.; Wiley-VCH: Germany, **2005**.
5. Auras, R. A.; Lim, L. T.; Selke, E. M.; Tsuji, H. In Poly(lactic acid): Synthesis, Structures, Properties, Processing, and Applications; Grossman, R F., Nwabunma, D., Eds.; Wiley: NJ, **2010**.
6. Garlotta, D. *Polym. Environ.* **2001**, *9*, 63.

7. Leenslag, J. W.; Pennings, A. J.; Bos, R. R. M.; Rozema, F. R.; Boering, G. *Biomaterials* **1987**, *8*, 311.
8. Penning, J. P.; Dijstra, H.; Pennings, A. J. *Polymer* **1993**, *34*, 942.
9. Vainiopa, S.; Rokkanen, P.; Tormala, P. *Prog. Polym. Sci.* **1989**, *14*, 679.
10. Singh, R. P.; Pandey, J. K.; Rutot, D.; Degée, P.; Dubois, P. *Carbohydr. Res.* **2003**, *338*, 1759.
11. Di, Y.; Iannace, S.; Di Maio, E.; Nicolais, L. *J. Polym. Sci. Part B: Polym. Phys.* **2005**, *43*, 689.
12. Okamoto, M. In Handbook of Biodegradable Polymeric Materials and Their Applications; Mallapragada, S.; Narasimhan, B., Eds.; Iowa State University: Ames, **2005**; Vol. 1, p 1.
13. Castrillo, P. D.; Olmos, D.; Amador, D. R.; González-Benito, J. *J. Colloid Interface Sci.* **2007**, *308*, 318.
14. Giannelis, E. P. *Appl. Organomet. Chem.* **1998**, *12*, 675.
15. Okada, A.; Kawasumi, M.; Usuki, A.; Kojima, Y.; Kurauchi, T.; Kamigaito, O. In Polymer Based Molecular Composites; Schaefer, W.; Mark, E., Eds.; MRS Symposium Proceedings: Pittsburgh, **1990**; Vol. 171, p 45.
16. Gilman, J. W. *Appl. Clay Sci.* **1999**, *15*, 31.
17. Messersmith, P. B.; Giannelis, E. P. J. *Polym. Sci. Part A: Polym. Chem.* **1995**, *33*, 1047.
18. Gilman, J. W.; Jackson, C. L.; Morgan, A. B.; Harris, R.; Manias, E.; Giannelis, E. P.; Wuthenow, M.; Hilton, D.; Phillips, S. H. *Chem. Mater.* **2000**, *12*, 1866.
19. Agubra, V. A.; Owuor, P. S.; Hosur, M. V. *Nanomaterials* **2013**, *3*, 550.
20. Olmos, D.; Domínguez, C.; Castrillo, P. D.; González-Benito, *J. Polym.* **2009**, *50*, 1732.
21. Serra, R.; González-Gaitano, G.; González-Benito, J. *Polym. Compos.* **2012**, *33*, 1549.
22. Olmos, D.; Martínez-Tarifa, J. M.; González-Gaitano, G.; González-Benito, J. *Polym. Test.* **2012**, *31*, 1121.
23. González-Benito, J.; Castillo, E.; Caldito, J. F. *Eur. Polym. J.* **2013**, *49*, 1747.
24. Matusik, J.; Stodolak, E.; Bahranowski, K. *Appl. Clay Sci.* **2011**, *51*, 102.
25. Konsomboon, S.; Pipatmanomai, S.; Madhiyanon, T.; Ti, S. *Appl. Energy* **2011**, *88*, 298.
26. Diniz Melo, J. D.; De Carvalho Costa, T. C.; De Medeiros, A. M.; Paskocimas, C. A. *Ceram. Int.* **2010**, *36*, 33.
27. Zhang, J.; Duan, Y.; Sato, H.; Tsuji, H.; Noda, I.; Yan, S.; Ozaki, Y. *Macromolecules* **2005**, *38*, 8012.
28. Pan, P.; Kai, W.; Zhu, B.; Dong, T.; Inoue, Y. *Macromolecules* **2007**, *40*, 6898.
29. Pan, P.; Zhu, B.; Kai, W.; Dong, T.; Inoue, Y. *Macromolecules* **2008**, *41*, 4296.
30. Worln, R. *Am. Mineral* **1963**, *48*, 390.
31. Castrillo, P. D. Preparación, caracterización y análisis de materiales nanocompuestos basados en sistemas epoxi-caolín, Ph.D. Thesis, Universidad Carlos III de Madrid, March **2010**.
32. Farmer, V. C. *Clay Minerals* **1998**, *33*, 601.
33. Matusik, J.; Kłapyta, Z.; Olejniczak, Z. *Appl. Clay Sci.* **2013**, *83–84*, 426.
34. Frost, R. L.; Makó, E.; Kristóf, J.; Kloprogge, J. T. *Spectrochim. Acta A Mol. Biomol. Spectrosc.* **2002**, *58*, 2849.
35. Arroyo, J. M.; Olmos, D.; Orgaz, B.; Puga, C. H.; San José, C.; González-Benito, J. *RSC Adv.* **2014**, *4*, 51451.